NIH Public Access
Author Manuscript
Neuroscience. Author manuscript; available in PMC 2006 May 24.

Published in final edited form as:
Neuroscience. 2006 May 12; 139(2): 597–607.

CELLULAR AND SUBCELLULAR LOCALIZATION OF PDE10A, A STRIATUM-ENRICHED PHOSPHODIESTERASE

Z. XIE[a], **W. O. ADAMOWICZ**[b], **W. D. ELDRED**[c], **A. B. JAKOWSKI**[d], **R. J. KLEIMAN**[b], **D. G. MORTON**[d], **D. T. STEPHENSON**[d], **C. A. STRICK**[b], **R. D. WILLIAMS**[b], and **F. S. MENNITI**[b,*]

a*Protein Sciences, Pfizer Global Research and Development, Eastern Point Road, Groton, CT 06340, USA*

b*CNS Discovery, Pfizer Global Research and Development, Eastern Point Road, Groton, CT 06340, USA*

c*Department of Biology, Boston University, Boston, MA 02215, USA*

d*Safety Sciences, Pfizer Global Research and Development, Eastern Point Road, Groton, CT 06340, USA*

*Corresponding author. Tel: +1-860-441-5939; fax: +1-860-686-0013. E-mail address: frank.s.menniti@pfizer.com (F. S. Menniti).

Abbreviations:

cAMP cyclic AMP

cGMP cyclic guanosine mono-phosphate

ChAT choline acetyl transferase

DAPI 4’,6-diamidino-2-phenylindole

DARPP-32 dopamine- and cyclic AMP-regulated phosphoprotein, M_r 32 kDa

n. nucleus

nNOS neuronal nitric oxide synthetase

PB 0.1 M phosphate buffer

PDE phosphodiesterase

PDE10A-ir PDE10A-like immunoreactivity

PSD postsynaptic densities

SPM synaptosomal membrane

SPS synaptic vesicle

SPV synaptosomal vesicle pellet.

NIH-PA Author Manuscript
NIH-PA Author Manuscript
NIH-PA Author Manuscript

NIH-PA Author Manuscript

NIH-PA Author Manuscript

NIH-PA Author Manuscript

Abstract

PDE10A is a recently identified phosphodiesterase that is highly expressed by the GABAergic medium spiny projection neurons of the mammalian striatum. Inhibition of PDE10A results in striatal activation and behavioral suppression, suggesting that PDE10A inhibitors represent a novel class of antipsychotic agents. In the present studies we further elucidate the localization of this enzyme in striatum of rat and cynomolgus monkey. We find by confocal microscopy that PDE10A-like immunoreactivity is excluded from each class of striatal interneuron. Thus, the enzyme is restricted to the medium spiny neurons. Subcellular fractionation indicates that PDE10A is primarily membrane bound. The protein is present in the synaptosomal fraction but is separated from the postsynaptic density upon solubilization with 0.4% Triton X-100. Immuno-electron microscopy of striatum confirms that PDE10A is most often associated with membranes in dendrites and spines. Immuno-gold particles are observed on the edge of the postsynaptic density but not within this structure. Our studies indicate that PDE10A is associated with post-synaptic membranes of the medium spiny neurons, suggesting that the specialized compartmentation of PDE10A enables the regulation of intracellular signaling from glutamatergic and dopaminergic inputs to these neurons.

Keywords

phosphodiesterase; CNS; striatum; medium spiny neurons; immunohistochemistry

Cyclic nucleotides play an important role as second messengers in the CNS. Concentrations of cyclic AMP (cAMP) and cyclic guanosine monophosphate (cGMP) are determined by the rate of synthesis, and of equal importance, by the rate of degradation by the phosphodiesterases (PDEs). The PDEs are a super family of enzymes encoded by 21 genes and subdivided into 11 distinct families according to structural, functional and kinetic properties (Soderling and Beavo, 2000). Most of the PDEs are differentially expressed within the CNS and many neurons appear to express multiple PDEs. This suggests that different isozymes subserve distinct physiological functions in different neuronal pathways and within individual neurons. Thus, an important step in elucidating these functions is mapping the differential localization of the PDEs within the CNS, both among different neuronal populations and at the subcellular level within identified neuronal types.

PDE10A is the single member of one of the newest PDE gene families. Initial characterization (Fujishige et al., 1999a; Loughney et al., 1999; Soderling et al., 1999) indicates that PDE10A is a dual-substrate PDE that is highly enriched in brain. Fujishige et al. (1999b) noted high expression in human caudate nucleus (n.) and putamen. Seeger et al. (2003) subsequently reported that in rat, PDE10A mRNA and protein are highly enriched in the GABAergic medium spiny projection neurons of the striatal complex (caudate n., n. accumbens, and olfactory tubercle), an expression pattern evident in other mammalian species (Coskran et al., 2005; Coskran et al., in preparation). The striatal complex forms the core of the basal ganglia, a system of interconnected nuclei that process cortical information in the context of dopaminergic signaling to regulate motoric, appetitive, and cognitive processes. Recently, papaverine was identified as a specific inhibitor of PDE10A (Siuciak et al., submitted for publication, 2005). Systemic administration of this compound to mice produces a rapid increase in striatal cGMP and cAMP along with downstream markers of activation of the protein kinase A/protein kinase G signaling cascades. Papaverine potentiates catalepsy produced by the dopamine D_2 receptor antagonist haloperidol in rats and inhibits conditioned avoidance responding in rats and mice. These findings suggest that inhibition of PDE10A may be a novel approach to the treatment of psychosis (Siuciak et al., submitted for publication, 2005; in press, 2006).

NIH-PA Author Manuscript

NIH-PA Author Manuscript

NIH-PA Author Manuscript

The behavioral effects of papaverine suggest that PDE10A regulates the excitability of medium spiny neurons (Siuciak et al., submitted for publication, 2005; in press ,2006). However, the excitability of these neurons is also regulated by several classes of aspiny striatal inter-neurons (Kawaguchi et al., 1995). Expression of PDE10A in one or more of these interneuron populations would have implications for understanding the mechanism by which this enzyme regulates striatal output. Thus, the first aim of the present studies was to determine whether PDE10A is expressed within any striatal interneurons in addition to the medium spiny projection neurons. It is also becoming increasingly clear that cyclic nucleotide signaling is highly compartmentalized within cells, indicating a mechanism whereby different PDE isozymes may sub-serve distinct physiological functions within a single cell (Houslay and Adams, 2003; Houslay and Milligan, 1997). Thus, the second aim of the present study was to investigate the subcellular distribution of PDE10A in the striatal medium spiny neurons, to provide further context for elucidating the mechanism(s) whereby the enzyme regulates the excitability of these neurons.

EXPERIMENTAL PROCEDURES

Animals

Male Sprague-Dawley rats (Charles River Laboratories, Kingston, NY, USA) weighing 300-400 g were housed in groups of five to 10 at ambient temperature of 25-27 °C, under a 12-h light/dark cycle. Food and water was available *ad libitum*. For preparation of samples for subcellular fractionation, rats were killed by decapitation. For preparation of samples for immunoelectron microscopy, rats were killed by overdose with 100 mg of pentobarbital prior to perfusion fixation. Cynomolgus monkeys (Charles River Primates, BRF, Houston, TX, USA) 2-3 years of age were housed singly in an AAALAC, International accredited animal facility, fed commercial monkey chow supplemented with fruit, provided unlimited access to water, and used as untreated control animals on pharmacokinetic and toxicology studies. Immediately prior to sample collection, monkeys were sedated with i.m. injections of ketamine, killed with i.v. injections of pentobarbital, and exsanguinated. All procedures relating to animal care and treatment were conducted according to the guidelines of the Institutional Animal Care and Use Committee at Pfizer, the ILAR Guide for the Care and Use of Laboratory Animals, and all federal and international regulations. All efforts were made to minimize the number of animals used and their suffering.

Western blot comparing rat and cynomolgus striatal extracts

Rat brains were collected after rapid decapitation and striatum was dissected using the atlas of Paxinos and Watson (1986) as a guide. Tissue was homogenized by sonication in lysis buffer B (50 mM Tris-HCl, pH 7.5, 250 mM NaCl, 5 mM EDTA, pH 8.0, 0.1% nonidet P-40 and complete protease inhibitors). The lysates were centrifuged at 11,650×*g* for 30 min at 4 °C. Pellets were discarded and supernatants stored at -80 °C. Cynomolgus monkey brains were collected and striatum was dissected using the atlas of Paxinos et al. (2000) as a guide. Tissue was homogenized in a glass Teflon dounce homogenizer using five volumes to weight B-Per extraction reagent containing complete protease inhibitors. Lysates were centrifuged at 11,650×*g* for 10 min at 4 °C. Pellets were discarded and supernatants stored at -80 °C. Protein concentrations in supernatants were determined by the bicinchoninic acid method (Pierce Chemical Co., Rockford, IL, USA). Equal amounts of striatal homogenates were resolved on 4-12% NuPAGE Bis-Tris gel (Invitrogen Corporation, Carlsbad, CA, USA) in MOPS buffer and transferred to nitrocellulose as described below in *Subcellular fractionation*.

Immunohistochemistry and confocal microscopy

Double immunofluorescence techniques were employed to investigate the localization of PDE10A relative to defined populations of striatal neurons in striatum of cynomolgus monkey.

NIH-PA Author Manuscript

NIH-PA Author Manuscript

NIH-PA Author Manuscript

The caudate and putamen from immersion fixed (10% neutral buffered formalin, 24 h duration fixation) cynomolgus monkey brain were processed according to routine histological procedures and embedded in paraffin wax. Six micron sections were collected on charged microscope slides, deparaffinized and hydrated to distilled water. Immunohistochemistry was performed using co-localization of two antibodies, derived from different species, on the same tissue section by sequential and simultaneous double immunofluorescence techniques. Immunohistochemistry conditions were optimized for each antibody on individual single-stained sections prior to dual staining. Control sections were stained with individual antibodies where one of the two antibodies was replaced with isotype control IgG from the appropriate species. Individual fluorophores and filter sets were chosen to eliminate the possibility of overlap of signal. Masked epitopes were retrieved using Antigen Retrieval Citra Solution (BioGenex, San Ramon, CA, USA) heated to 96 °C with a steamer for 20 min followed by cooling for 20 min at room temperature. Brain sections were incubated with the PDE10A mouse monoclonal antibody 24F3.F11 diluted 1:250 for 60 min at room temperature. PDE10A-like immunoreactivity (PDE10A-ir) was detected using a biotinylated secondary antibody, horse anti-mouse IgG (BA-2000; 1:150, Vector Laboratories, Burlingame, CA, USA), and visualized with Alexa 488-Streptavidin (Invitrogen Corporation). Sections stained with 24F3.F11 were then incubated for 24 -48 h at 4 °C with antibodies to dopamine- and cyclic AMP-regulated phosphoprotein, M_r 32 kDa (DARPP-32) (# 2302, 1:50, Cell Signaling Technology, Inc., Beverly, MA, USA), calretinin (AB1550, 1:1000; Chemicon International Inc., Temecula, CA, USA), parvalbumin (Ab-1, PC255L; 1:500; Oncogene Science, Cambridge, MA, USA) or choline acetyltransferase (AB144P; 1:500; Chemicon International Inc.). Interneuronal markers were visualized by labeling with goat anti-rabbit antibody directly conjugated to Alexa 568 (1:200). Antibody to neuronal nitric oxide synthase (AB5380; 1:1000; Chemicon International Inc.) was co-incubated with 24F3.F11 (1:250) overnight at 4 °C and visualized with a cocktail of directly labeled secondary antibodies (1:200), goat anti-rabbit-Alexa 568 and goat anti-mouse-Alexa 488, respectively. Nuclei were stained with 4’ ,6-diamidino-2-phenylindole (DAPI; Invitrogen Corporation). Images of PDE10A plus parvalbumin-stained sections were acquired on a Leica TCS-SP laser scanning confocal microscope (Leica Microsystems Inc., Exton, PA, USA) equipped with argon, krypton, and UV lasers, which allowed excitation at 488, 568, and 358 nm wavelengths for the detection of Alexa 488, Alexa 568, and DAPI, respectively. The Alexa 488 dye yields a green signal, Alexa 568 is red and DAPI is blue when visualized with the appropriate fluorescent filters. The DARPP-32 plus PDE10A-stained images were photographed with a Zeiss Axioplan microscope equipped with an AxioCam HR digital camera (Carl Zeiss MicroImaging, Inc., Thornwood, NY, USA) and the PDE10A plus neuronal nitric oxide synthetase (nNOS), choline acetyl transferase (ChAT) and calretinin dual-stained sections were photographed on a Nikon Eclipse E800 microscope equipped with a SpotRT camera (Maeger Scientific, Dexter, MI, USA). Each fluorescent channel was acquired sequentially and then merged to create the final image.

Immunoelectron microscopy

Pentobarbital-overdosed rats were perfused with 200 ml of saline (0.9%) followed by 250 ml of 4% paraformaldehyde with 0.1% glutaraldehyde pH 7.4 in 0.1 M phosphate buffer (PB). The brains were removed and block cut to expose the ventricles, then post-fixed for 30 min in the same para/glut perfusate, and finally post-fixed for 3h in 4% paraformaldehyde (no glut) pH 10.1 at room temperature on a rotator. Following cryoprotection using an ascending sucrose series, a sliding microtome was used to cut 60-75 μm thick frozen coronal sections. Following a descending sucrose series into PB, the sections were treated with fresh 1% sodium borohydride in PB for 30 min. The sections were then washed in PB and transferred into 24F3.F11 diluted 1:2000 in PB for 48 h. Control sections were incubated in the absence of 24F3.F11. Following 3×30 min washes in PB, the sections were transferred to goat anti-mouse FAB Nanogold secondary antibody (Nanoprobes, Inc., Yaphank, NY, USA) diluted 1:100 in

NIH-PA Author Manuscript

NIH-PA Author Manuscript

NIH-PA Author Manuscript

PB with 0.5% bovine serum albumin at 4 °C and incubated on a rotator for 72 h. After several 15 min PB rinses, the sections were post-fixed with 1% glutaraldehyde in PB for 45 min. Following several changes of PB, the sections were silver intensified and gold toned (Nanoprobes, Inc.) before fixation in 1% OsO_4 in PB for 45 min. The sections were then incubated in 1% uranyl acetate in 30% acetone for 30 min, dehydrated using an acetone series, and embedded in epoxy resin. Thin sections were examined unstained using a JEOL 2010 electron microscope.

Subcellular fractionation

Subcellular fractionation was carried out as described by Blackstone et al. (1992). Brain tissue from six rats was homogenized in 20 volumes of lysis buffer (0.32 M sucrose, 4 mM HEPES/NaOH, pH 7.4, 5 mM DTT, 1 mM EDTA, and Complete protease inhibitor tablets) with a glass-Teflon homogenizer. The homogenate was centrifuged at 800×*g* to yield P0 and S0. The pellet, P0, was washed in five volumes of lysis buffer, centrifuged again to yield P1 and S1. P1, containing crude nuclear pellet and unbroken cells, was discarded. S0 and S1 were pooled and centrifuged at 9000×*g* yielding S2 and a crude synaptosomal fraction (P2). P2 was washed in 10 volumes lysis buffer to yield a washed synaptosomal fraction (P2') and S2'.P2' was lysed by hypo-osmotic shock using a 25G needle to resuspend the pellet in three volumes of water. The lysed synaptosomal fraction was adjusted to 1 mM HEPES, pH 7.5 and rocked at 4 °C for 30 min. The lysate was centrifuged at 25,000×*g* for 20 min to yield crude synaptosomal membranes (SPM) and synaptic vesicles (SPS). The crude SPM were resuspended in six volumes lysis buffer and loaded onto a sucrose step gradient containing 0.8 M sucrose 1.0 M, and 1.2 M sucrose in 0.5 mM HEPES (pH 7.4) 5 mM DTT, 1 mM EDTA and complete protease inhibitor tables. The gradient was centrifuged for 2h at 65,000×*g* in a Beckman SW-28 rotor. Fractions were collected from the 0.8 M/1.0 M layer (SPM2), and at the 1.0 M/1.2 M interface (SPM4), with a crude mitochondrial pellet at the bottom of the tube. The SPM2 and crude mitochondrial pellet were resuspended directly in SDS sample buffer (Invitrogen). According to Blackstone et al. (1992) the SPM4 is the synaptosomal plasma membrane fraction, from which postsynaptic densities (PSDs) were isolated. The SPM4 were collected by centrifugation at 100,000×*g* for 1 h and washed once with lysis buffer. The washed membranes were solubilized with 0.4% Triton X-100 in 0.5 mM HEPES (pH 7.4) for 1h at4°C and then centrifuged at 100,000×*g* for 1 h. The resulting pellet was washed once in 0.4% Triton extraction buffer and once again in lysis buffer. The pellet containing the PSD and the soluble fractions were analyzed separately.

The supernatant S2 was further spun at 100,000×*g* using the Beckman TLA 100.2 rotor to yield the high speed membrane fraction P20. P20 was resuspended into lysis buffer and further incubated either with no addition, or with the addition of (final concentrations) 1 M NaCl, 0.4% Triton X-100, or 0.1 M Na_2CO_3 (pH 10) for 10 min on ice. The suspensions were then spun for 1 h at 100,000×*g* using the Beckman TLA 100.2 rotor. The resulting pellets were washed, resuspended in lysis buffer and analyzed by Western blotting along with the supernatant fractions.

Samples were taken at various steps during the subcellular fractionation and loaded by equal volumes, adjusting for resuspension volumes, for analysis by Western blotting using the Invitrogen NuPage system with detection using a LiCor Odyssey or with ECL Detection System (Amersham Biosciences, Piscataway, NJ, USA). Samples were prepared using NuPage LDS sample buffer and run on 4-12% gels with MOPS or MES buffer and then transferred to 0.45 μM pore nitrocellulose membrane. Blots were blocked in Odyssey block followed by incubation in primary and secondary antibody in 50% Odyssey block with 0.1% Tween-20 in PBS. Washes were carried out in 0.1% Tween-20 in PBS. The antibodies and titers employed were: PDE10A mouse monoclonal antibody 24F3.F11 (1:1000); the plasma membrane marker,

NIH-PA Author Manuscript

NIH-PA Author Manuscript

NIH-PA Author Manuscript

sodium potassium ATPase antibody # ab7671 from Abcam (Cambridge, MA, USA; 1:1000); PSD95 mouse monoclonal antibody MA1-045 from Affinity Bioreagents (Golden, CO, USA; 1:2000); NMDAR1 mouse monoclonal antibody 3556308 from BD Pharmingen (San Diego, CA, USA; 1:2000); rabbit polyclonal anti-DARPP-32 antibody from Chemicon (1:1000); synaptophysin mouse monoclonal RDI-PRO61012 from Research Diagnostics (Concord, MA, USA; 1:1000); polyclonal PDE2A antibody PD2A-100P from Fabgennix (Frisco, TX, USA; 1:1000); PDE1B1 antibody # AB1655 from Chemicon (1:1000). Alexa 680 Fluorescent anti-mouse and anti-rabbit secondary antibodies were purchased from Molecular Probes (Eugene, OR, USA) and used at a dilution of 1:2000. IRdye 800 secondary antibodies from Rockland Immunochemicals (Gilbertsville, PA, USA) to mouse and rabbit were diluted 1:5000; horseradish peroxidase-conjugated anti-rabbit secondary antibody (Cell Signaling) at 1:5000 dilution.

RESULTS

PDE10A is expressed only in striatal medium spiny projection neurons

The medium spiny projection neurons that express PDE10A are the major neuronal type in striatum. However, there are several classes of striatal interneurons that play a major role in organizing the activity of the medium spiny neurons (Kawaguchi et al., 1995). Thus, it is of interest to determine whether PDE10A is also expressed in any of the interneuron subtypes. This was investigated using immunofluorescent double staining to compare the disposition of PDE10A protein with that of a marker for the medium spiny neurons (DARPP-32; Greengard et al., 1999) and each of the interneuron classes. Specifically, interneuron populations were labeled with antibodies to nNOS, calretinin, ChAT, and parvalbumin.

Double labeling immunohistochemical analyses for PDE10A and the four interneuron markers were carried out in both rat and cynomolgus monkey striatum. We have observed that the localization pattern of PDE10A in the brain is very similar across mammalian species including mouse, rat, dog, cynomolgus monkey and human (Coskran et al., 2005; Coskran et al., in preparation). We chose to use cynomolgus monkey brain for presentation of the double labeling in the present study for several reasons. In rat, PDE10A immunoreactivity in striatum is of very similar intensity in the cell bodies of the medium spiny neurons and in the neuropil. In contrast in cynomolgus striatum, the intensity of PDE10A immunoreactivity in the medium spiny neuron cell bodies is notably greater than that of the surrounding neuropil. This allows for an easier visualization of neuronal cell bodies for double labeling with interneuron markers. Nonetheless, the results of the double labeling immunohistochemical analyses for PDE10A and the four interneuron markers in rats were qualitatively similar to those described here for cynomolgus monkey (unpublished observations). PDE10A-ir was detected with the mouse monoclonal antibody 24F3.F11 (Seeger et al., 2003). The specificity of this antibody for PDE10A in cynoognizes a single band of approximately 89 kDa in cynomolgus monkey striatal extract. The molecular size of this band and the intensity of immunoreactivity are similar to that observed in an equivalent amount of rat striatal tissue extract. Omitting 24F3.F11 or primary antibody for each of the interneuron markers abolished staining, also supporting specificity of staining (data not shown).

In cynomolgus monkey, dense PDE10A-ir is observed throughout the striatum, including the vast majority of the cell bodies and the parenchyma (Figs. 1 A, 1B and 2A), as in rat (Coskran et al., 2005;Seeger et al., 2003; Coskran et al., in preparation). The pattern of PDE10A-ir was indistinguishable in samples derived from four monkeys, thus, further detailed analysis using dual labeling was carried out on samples derived from a single animal. There was a complete overlap between cell bodies expressing DARPP-32-like immunoreactivity and PDE10A-ir (Fig. 1A and 1B). This pattern of labeling with 24F3.F11 is interpreted to indicate that PDE10A

NIH-PA Author Manuscript

NIH-PA Author Manuscript

NIH-PA Author Manuscript

is expressed in the majority of the medium spiny projection neurons, including the dendritic arbors of these neurons (Seeger et al., 2003).

An antibody to nNOS labeled the cell bodies and main dendritic branching of a rare subset of neurons within cynomolgus monkey striatum (Fig. 2B and 2C). In double stained sections, the neurons labeled with the nNOS antibody were completely devoid of PDE10A-ir (Fig. 2C). Antibodies to calretinin, ChAT, and parvalbumin were used to identify three additional interneuron populations. Again, each antibody labeled the cell bodies of small cell populations (Fig. 1D-F). In each case, there was no overlap with PDE10A-ir (Fig. 1D-F). The lack of co-localization between PDE10A-ir and parvalbumin-like immunoreactivity is highlighted in the confocal image illustrated in Fig. 1F. The Ortho-Slice function in the Leica confocal software allowed simultaneous visualization of a point of interest from an image stack in both the y-z plane and x-z plane. This point of interest in Fig. 1F, a single parvalbumin-labeled cell body (red), shows virtually no signal overlap between PDE10A-ir (green) and parvalbumin-like immunoreactivity (red), thereby confirming the lack of co-localization. Similar results were observed using rat striatum (unpublished observations). These results indicate that PDE10A is not expressed in the different interneuron populations within the striatum.

Subcellular distribution of PDE10A-biochemical analysis

Given that the majority of the neurons in the striatum are the medium spiny projection neurons, and that these neurons appear to be the only population expressing PDE10A, we next investigated the subcellular distribution of PDE10A in the medium spiny neurons using classical differential centrifugation techniques on rat striatal homogenates. The differential centrifugation scheme employed is illustrated in Fig. 3. The qualitative distribution of PDE10A in the fractions isolated using this scheme is indicated (red). Similar results were obtained in three separate experiments, although not all fractions were analyzed in each experiment.

Striatal homogenate was first centrifuged at 800×*g*. The supernatant (S1) was then fractionated by centrifugation at 9000×*g* to isolate a crude synaptosomal vesicle pellet (SPV). Western blot analysis with 24F3.F11 indicates that approximately 50% of the PDE10A-ir was recovered in the SPV and 50% remained in the supernatant (S2; Fig. 4). Further centrifugation of S2 at 100,000×*g* followed by Western blotting indicated that the majority of the PDE10A-ir was recovered in the pellet (see Fig. 6). The SPV was lysed by resuspension in hypotonic buffer and then fractionated by centrifugation at 25,000×*g*. PDE10A-ir was recovered in the SPM fraction but was not detectable in the SPS. The SPM was then resuspended and resolved on a sucrose step gradient into three fractions: SPM2 containing myelin sheets, SPM4 containing the PSD, and a pellet containing mitochondria and other insoluble material (SPMB). PDE10A-ir loaded onto this gradient was recovered in all three fractions (SPM4, Fig. 5; SPM2 and SPMB, data not shown).

To investigate whether PDE10A is tightly associated with the signaling complexes of the PSD, a PSD containing fraction (SPM4) was isolated from the SPM using a sucrose step gradient. Upon solubilization of SPM4 with Triton X-100 and centrifugation, both PSD-95- and NMDAR1-like immunoreactivity were recovered in the pellet (Fig. 5), as previously reported (Kim and Sheng, 2004). In contrast, PDE10A-ir, was recovered exclusively in the soluble fraction (SPM4S).

The distribution of PDE10A-ir was also compared with that of a number of proteins used as markers for different subcellular compartments (Fig. 4). PDE10A-ir had a distribution similar to that of the plasma membrane associated Na^+/K^+ ATPase and PSD95. This distribution differed from that of DARPP-32, which was detected in the S2 but not in the subsequent SPV. This distribution of DARPP-32 is consistent with the previous reports that the protein is cytosolic (Greengard et al., 1999;Hemmings et al., 1984). The distribution of PDE10A-ir was

NIH-PA Author Manuscript

NIH-PA Author Manuscript

NIH-PA Author Manuscript

also distinct from that of synaptophysin, an integral membrane glycoprotein associated with presynaptic nerve terminals vesicles (Wiedenmann and Franke, 1985). Like PDE10A-ir, synaptophysin-like immunoreactivity was observed in the SPV fraction. Upon hypotonic lysis of the SPV fraction, synaptophysin-like immunoreactivity was recovered primarily in the soluble fraction SPS, which presumably contains the presynaptic neurotransmitter vesicles. In contrast, PDE10A-ir was recovered primarily in the membrane fraction SPM.

There are several PDEs that are also highly expressed in the striatal medium spiny neurons, including PDE1B (Repaske et al., 1993) and PDE2 (Van Staveren et al., 2003) and we compared the distribution of these enzymes to that of PDE10A. PDE2-like immunoreactivity had a distribution similar to that of PDE10A with one exception. Like PDE10A-ir, PDE2-like immunoreactivity was observed in the SPV, and SPM fractions. However, PDE2-like immunoreactivity was also observed in SPS, in contrast to PDE10A-ir. After sucrose gradient density fractionation of SPM, PDE2-like immunoreactivity was recovered in SPM4 and, like PDE10A, was nearly completely excluded from the Triton-insoluble PSD fraction. In contrast to PDE10A and PDE2, PDE1B-like immunoreactivity was observed almost exclusively in soluble fractions. Thus, the distribution of PDE1B-like immunoreactivity was very similar to that of DARPP-32.

The mechanism of membrane association of PDE10A was also investigated. The S2 fraction was centrifuged at high speed (100,000×*g*) to obtain the P20 membrane fraction, which was then solubilized under different conditions and centrifuged again. As shown in Fig. 6, PDE10A-ir was recovered in the supernatant fraction following incubation of P20 with 0.4% Triton X-100. In contrast, PDE10A-ir remained in the pellet in incubations containing 1 M NaCl or 0.1 M Na2CO3 (pH 10). Purified rat recombinant PDE10A incubated with each of these solubilization buffers and then centrifuged was recovered in the supernatant. Thus, recovery of the native PDE10A in pelleted fraction is unlikely due to artifactual protein precipitation. These results suggest that PDE10A associates with membranes through a non-ionic interaction.

Subcellular distribution of PDE10A-immunoelectron microscopy

The results of the biochemical subcellular fractionation studies described above indicate that PDE10A is primarily membrane associated in the medium spiny neurons. Our previous study in rat (Seeger et al., 2003) and the results presented in Fig. 1 from cynomolgus monkey indicate that the enzyme is distributed throughout the dendritic compartment of these neurons. However, it appears that PDE10A is not tightly associated with the PSD. Thus, to gain greater insight into the distribution of PDE10A in the dendritic compartment, we evaluated the distribution of PDE10A in rat striatum by immunoelectron microscopy.

Fig. 7 is representative images of the distribution of gold particles in 24F3.F11-labeled sections of rat striatum capturing a number of vesicle-filled nerve terminals (P) of presumed glutamatergic striatal afferents as well as dendrites (D) and spines (S) of presumed medium spiny neurons. The majority of gold particles are observed in close apposition to membranes of dendrites and spines (blue arrows). Particles are also observed within spines not obviously associated with a membrane (red arrows). Interestingly, particles are observed at the edge of PSDs (yellow arrows) but not directly apposed to these structures. Particles are not observed associated with vesicle-filled presynaptic terminals. Finally, in samples from which the primary antibody was omitted during processing for immunoelectron microscopy, virtually no silver grains were detected, indicating the specificity of the immunolabeling (data not shown).

DISCUSSION

PDE10A is highly enriched in the mammalian striatum (Coskran et al., 2005; Seeger et al., 2003; Coskran et al., in preparation; and present study) and specifically in the GABAergic

NIH-PA Author Manuscript

NIH-PA Author Manuscript

NIH-PA Author Manuscript

medium spiny projection neurons that are the major neuronal cell type in this brain region. The medium spiny neurons are the principal input site for the basal ganglia circuit (Wilson, 1998). These neurons receive a massive excitatory input from cortical and thalamic glutamatergic neurons and are also the principal recipient of the rostral projection of the midbrain dopaminergic neurons. The medium spiny neurons integrate this cortical/thalamic information in the context of dopaminergic signaling, and reflect this output as a single burst or short bursts of action potentials from these typically quiescent neurons. Thus, the regulation of medium spiny neuron excitability is a key element in regulating information processing by the basal ganglia complex. Recent results utilizing a PDE10A inhibitor and genetic inactivation of PDE10A suggest that this enzyme plays a critical role in regulating the excitability of these neurons. Papaverine has been identified as a specific inhibitor of PDE10A, enabling an investigation of the behavioral effects of inhibiting this enzyme in rodents (Siuciak et al., submitted for publication, 2005). PDE10A inhibition with papaverine potentiates haloperidol-induced catalepsy in rats, inhibits conditioned avoidance responding in mice (Siuciak et al., submitted for publication, 2005), and inhibits the locomotor hyperactivity induced by stimulants (Schmidt et al., 2003). The PDE10A knockout mice exhibit reduced locomotor activity when introduced into a novel environment and also have a reduced locomotor stimulatory response to the NMDA receptor antagonist PCP but no change in response to amphetamine (Siuciak et al., in press, 2006). Thus, the behavioral effects of papaverine and the behavioral phenotype of the PDE10A knockout mice lead us to hypothesize that PDE10A inhibition results in an activation of striatal output leading to suppression of behavioral responsiveness (Siuciak et al., submitted for publication, 2005; in press, 2006). We are currently investigating the molecular mechanisms by which inhibition of PDE10A accounts for the hypothesized changes in striatal output. The present study provides several additional pieces of information that extends this investigation.

First, it is reported that PDE10A is expressed within the striatum exclusively by the medium spiny projection neurons and not in the different populations of striatal inter-neurons. Striatal interneurons play a key role in regulating the activity of medium spiny neurons (Kawaguchi, 1997; Kawaguchi et al., 1995). If PDE10A were expressed in one or more of these interneuron populations, then inhibition of interneuronal PDE10A might be expected to yield additional levels of regulation impinging upon medium spiny neuron output via interneuronal synaptic activity. Thus, we investigated whether PDE10A is expressed in the inter-neuron populations. Using double fluorescence immunohistochemistry and confocal microscopy in cynomolgus monkey striatum, no observable PDE10A expression was detectable in any of the four classes of striatal interneurons that are characterized by expression of nNOS, calretinin, ChAT, or parvalbumin. Instead, the expression of PDE10A in cell bodies overlaps with that of DARPP-32, which is a signaling molecule also highly expressed in striatal medium spiny neurons across mammalian species (Green-gard et al., 1999). Similar observations were made in rat striatum (unpublished observations). These results indicate that PDE10A is expressed exclusively by the medium spiny projection neurons within the striatum. Therefore, the effect of PDE10A inhibition on striatal output results from effects intrinsic to the medium spiny neurons.

In the medium spiny neurons, PDE10A was found to be highly enriched in membrane fractions during classical subcellular fractionation. PDE10A-ir in the cleared homogenate from rat striatum (S1) was recovered in the SPV along with the plasma membrane-associated Na^+/K^+ ATPase, and the synapse-associated proteins PSD95 and synaptophysin. In contrast, the cytosolic protein DARPP-32 was excluded from the SPV fraction. Upon hypotonic lysis of the synaptosomal fraction, both PDE10A and PSD95 remained in association with the membrane fraction, whereas synaptophysin was recovered in the supernatant, presumably associated with presynaptic neurotransmitter vesicles (Wiedenmann and Franke, 1985). A sucrose density step gradient was then used to isolate a fraction enriched in the PSD complex. This complex contains

NIH-PA Author Manuscript

NIH-PA Author Manuscript

NIH-PA Author Manuscript

a number of tightly associated proteins that are involved in the postsynaptic signaling response to glutamate (Kim and Sheng, 2004; Sheng and Sala, 2001). Upon Triton X-100 solubilization, PDE10A-ir was completely separated from PSD95 and NMDA receptor-like immunoreactivity (Kornau et al., 1995). These results indicate that PDE10A is highly associated with membranes from the medium spiny neurons but is not apparently an integral part of the PSD complex of these neurons.

Analysis of the distribution of PDE10A-ir using immunoelectron microscopy confirms and extends the above conclusion. In dendrites of medium spiny neurons, PDE10A-ir was primarily found apposed to membranes. In spines, the majority of the PDE10A-ir was also found in apparent association with membranes. However, PDE10A-ir was also observed with no clear membrane association. Immunoreactivity was not observed within the electron dense region characteristic of the PSD. However, it was not uncommon to observe gold particles at the edges of these structures. Thus, PDE10A is apparently contained within the spines of the medium spiny neurons, suggesting that the enzyme is appropriately compartmentalized to regulate postsynaptic cyclic nucleotide signaling and limit cyclic nucleotide accumulation near dendritic membranes.

The present results corroborate and extend the findings of Kotera et al. (2004). This group reported that PDE10A is primarily membrane associated in rat brain. Expression of PDE10A isoforms in PC12 cells suggested that membrane association depends on a unique n-terminal fragment of the PDE10A2 splice variant, the primary isoform of PDE10A expressed in rat striatum. Whereas in the PC12 cells, PDE10A2 appears to be localized primarily to membranes of the Golgi apparatus, the present results indicate that in medium spiny neurons membrane association extends to dendrites and spines. The results of the present study suggest that PDE10A associates with membrane through a hydrophobic interaction, since the protein is solubilized by treatment of membranes with Triton X-100 but remains membrane associated during treatment with high salt (Fig. 6). We also observed that PDE10A remained associated with membranes following treatment with Na2CO3. Resistance to solubilization by alkaline carbonate classifies PDE10A as an ‘integral’ membrane protein (Schwab et al., 2000). A single potential transmembrane region for rat PDE10A2, at amino acids 198-214, is predicted by the PSORT program for subcellular localization signals (Nakai and Horton, 1999). This region may contribute to the apparently tight association of PDE10A with membranes, but this remains to be determined.

Kotera et al. (2004) reported compelling evidence that the association of PDE10A with membranes may be regulated by n-terminal phosphorylation by PKA. Interestingly, we find in the present study through visualization by electron microscopy that the compartment where PDE10A may not be membrane associated is in spines. An intriguing speculation is that the activity of PDE10A is regulated by PKA (or PKG) phosphorylation primarily in the spines. The veracity of this speculation and the consequence of such redistribution for the regulation by PDE10A of signaling within the spines await further study.

There are a number of PDEs that are highly expressed in striatum in addition to PDE10A. These include two other isozymes, PDE1B (Repaske et al., 1993) and PDE2 (Van Staveren et al., 2003), that, like PDE10A, are capable of hydrolyzing both cAMP and cGMP. It is becoming increasingly apparent that expression of multiple PDE isoforms in a given cell population is common and that these different isoforms subserve distinct roles in the regulation of intracellular signaling cascades. Such segregation of functional activity for enzymes with seemingly identical catalytic activities occurs, at least in part, by differential subcellular distribution and compartmentation (Conti, 2000; Conti et al., 2003; Houslay et al., 2003). Thus, it was of interest to begin to investigate the possibility of differences in the subcellular distribution of PDE10A compared with PDE1B and PDE2 in striatum. The subcellular

NIH-PA Author Manuscript

NIH-PA Author Manuscript

NIH-PA Author Manuscript

distribution of PDE1B is clearly distinct from that of PDE10A. PDE1B-like immunoreactivity was recovered almost exclusively in the soluble fraction of the striatal extracts, similar to what was observed for the cytosolic signaling molecule DARPP-32 (Hemmings et al., 1984). Interestingly, the phenotype of PDE1B knockout mice appears to be distinctly different from that of the PDE10A knockout mice. Whereas the PDE1B knockout mice have a hyperlocomotor phenotype (Reed et al., 2002), the PDE10A knockout mice are characterized as exhibiting a hypolocomotor phenotype (Siuciak et al., in press, 2006). PDE1B knockout is associated with an increased phosphorylation of DARPP-32 at the PKA-regulated site, leading to the suggestion that PDE1B plays a role in the regulation of dopamine signaling in the striatum. It will be of interest to investigate the effects, if any, of PDE10A inhibition on DARPP-32 phosphorylation and signaling through this cascade. The subcellular distribution of PDE2 appears to be distinct from that of both PDE10A and PDE1B. Like PDE10A, PDE2 is membrane associated during subcellular fractionation. However, PDE2-like immunoreactivity was detected in the soluble fraction following lysis of the synaptosomal pellet, in contrast to PDE10A. The cellular distribution of PDE2 in the CNS appears to be more widespread than that of PDE10A, including expression in cortical neurons (Van Staveren et al., 2003). Thus, it is possible that the PDE2-like immuno-reactivity recovered in the synaptosomal supernatant may have originated in cortical neurons projecting into the striatum.

CONCLUSION

In summary, the present study indicates that PDE10A is localized exclusively in the medium spiny projection neurons of the mammalian striatum. In these neurons, the enzyme is associated with dendrites and spines but is not tightly associated with the signaling complex of the PSD. Other studies (Siuciak et al., submitted for publication, 2005; in press, 2006) suggest that PDE10A plays a role in regulating the excitability of the medium spiny neurons. The findings presented here begin to elucidate the signaling compartment through which PDE10A regulates the excitability of these neurons.

REFERENCES

Blackstone CD, Moss SJ, Martin LJ, Levey AI, Price DL, Huganir RL. Biochemical characterization and localization of a non-N-methyl-D-aspartate glutamate receptor in rat brain. J Neurochem 1992;58:1118–1126. [PubMed: 1371146]

Conti M. Phosphodiesterases and cyclic nucleotide signaling in endocrine cells. Mol Endocrinol 2000;14:1317–1327. [PubMed: 10976911]

Conti M, Richter W, Mehats C, Livera G, Park JY, Jin C. Cyclic AMP-specific PDE4 phosphodiesterases as critical components of cyclic AMP signaling. J Biol Chem 2003;278:5493–5496. [PubMed: 12493749]

Coskran, TM.; Jakowski, AB.; Ramirez, AD.; Morton, DG.; Menniti, FS.; Schmidt, CJ.; Kleiman, RJ.; Ryan, AM.; Stephenson, D. PDE10A: a CNS specific cGMP phosphodiesterase that is expressed in medium spiny neurons from multiple species. Society for Neuroscience 32nd annual meeting; 2005.

Fujishige K, Kotera J, Michibata H, Yuasa K, Takebayashi S, Okumura K, Omori K. Cloning and characterization of a novel human phosphodiesterase that hydrolyzes both cAMP and cGMP (PDE10A). J Biol Chem 1999a;274:18438–18445. [PubMed: 10373451]

Fujishige K, Kotera J, Omori K. Striatum- and testis-specific phosphodiesterase PDE10A isolation and characterization of a rat PDE10A. Eur J Biochem 1999b;266:1118–1127. [PubMed: 10583409]

Greengard P, Allen PB, Nairn AC. Beyond the dopamine receptor: the DARPP-32/protein phosphatase-1 cascade. Neuron 1999;23:435–447. [PubMed: 10433257]

Hemmings HC Jr, Nairn AC, Aswad DW, Greengard P. DARPP-32, a dopamine- and adenosine 3':5'-monophosphate-regulated phosphoprotein enriched in dopamine-innervated brain regions. II. Purification and characterization of the phosphoprotein from bovine caudate nucleus. J Neurosci 1984;4:99–110. [PubMed: 6319628]

NIH-PA Author Manuscript

NIH-PA Author Manuscript

NIH-PA Author Manuscript

Houslay MD, Adams DR. PDE4 cAMP phosphodiesterases: modular enzymes that orchestrate signalling cross-talk, desensitization and compartmentalization. Biochem J 2003;370:1–18. [PubMed: 12444918]

Houslay MD, Milligan G. Tailoring cAMP-signalling responses through isoform multiplicity. Trends Biochem Sci 1997;22:217–224. [PubMed: 9204709]

Kawaguchi Y. Neostriatal cell subtypes and their functional roles. Neurosci Res 1997;27:1–8. [PubMed: 9089693]

Kawaguchi Y, Wilson CJ, Augood SJ, Emson PC. Striatal interneurones: chemical, physiological and morphological characterization. Trends Neurosci 1995;18:527–535. [PubMed: 8638293]

Kim E, Sheng M. PDZ domain proteins of synapses. Nat Rev Neurosci 2004;5:771–781. [PubMed: 15378037]

Kornau HC, Schenker LT, Kennedy MB, Seeburg PH. Domain interaction between NMDA receptor subunits and the postsynaptic density protein PSD-95. Science 1995;5231:1737–1740. [PubMed: 7569905]

Kotera J, Sasaki T, Kobayashi T, Fujishige K, Yamashita Y, Omori K. Subcellular localization of cyclic nucleotide phosphodiesterase type 10A. J Biol Chem 2004;279:4366–4375. [PubMed: 14604994]

Loughney K, Snyder PB, Uher L, Rosman GJ, Ferguson K, Florio VA. Isolation and characterization of PDE10A, a novel human 3',5'-cyclic nucleotide phosphodiesterase. Gene 1999;234:109–117. [PubMed: 10393245]

Nakai K, Horton P. PSORT: a program for detecting sorting signals in proteins and predicting their subcellular localization. Trends Biochem Sci 1999;24:34–35. [PubMed: 10087920]

Paxinos, G.; Huang, X-F.; Toga, AW. The rhesus monkey brain in stereotaxic coordinates. Academic Press; San Diego: 2000.

Paxinos, G.; Watson, C. The rat brain in stereotaxic coordinates. Academic Press, Inc; San Diego: 1986.

Reed TM, Repaske DR, Snyder GL, Greengard P, Vorhees CV. Phosphodiesterase 1B knock-out mice exhibit exaggerated loco-motor hyperactivity and DARPP-32 phosphorylation in response to dopamine agonists and display impaired spatial learning. J Neurosci 2002;22:5188–5197. [PubMed: 12077213]

Repaske DR, Corbin JG, Conti M, Goy MF. A cyclic GMP-stimulated cyclic nucleotide phosphodiesterase gene is highly expressed in the limbic system of the rat brain. Neuroscience 1993;56:673–686. [PubMed: 8305078]

Schmidt CJ, Chapin DS, McCarthy SA, Fujiwara RA, Shrikhande A, Chambers L, Wong SF, Siuciak JA. The neurochemical and behavioral effects of papaverine in vivo suggest PDE10 inhibition is "antipsychotic.". Schizophr Res 2003;60:114.

Schwab RB, Okamoto T, Scherer PE, Lisanti MP. Analysis of the association of proteins with membranes. Curr Protoc Cell Biol 2000;5 4:1–17.

Seeger TF, Bartlett B, Coskran TM, Culp JS, James LC, Krull DL, Lanfear J, Ryan AM, Schmidt CJ, Strick CA, Varghese AH, Williams RD, Wylie PG, Menniti FS. Immunohistochemical localization of PDE10A in the rat brain. Brain Res 2003;985:113–126. [PubMed: 12967715]

Sheng M, Sala C. PDZ domains and the organization of supramolecular complexes. Annu Rev Neurosci 2001;24:1–29. [PubMed: 11283303]

Siuciak JA, Chapin DS, Harms JF, Lebel LA, McCarthy SA, Chambers L, Shrikhande A, Wong SF, Menniti FS, Schmidt CJ. The striatum-enriched phosphodiesterase PDE10A: role in regulation of basal ganglia output. J Neurosci. 2005submitted for publication

Siuciak JA, McCarthy SA, Chapin DS, Fujiwara RA, James LC, Williams RD, Stock JL, McNeish JD, Strick CA, Menniti FS, Schmidt CJ. Genetic deletion of the striatum-enriched phosphodiesterase PDE10A: evidence for altered striatal function. Neuropharmacol. 2006in press

Soderling SH, Bayuga SJ, Beavo JA. Isolation and characterization of a dual-substrate phosphodiesterase gene family: PDE10A. Proc Natl Acad Sci U S A 1999;96:7071–7076. [PubMed: 10359840]

Soderling SH, Beavo JA. Regulation of cAMP and cGMP signaling: new phosphodiesterases and new functions. Curr Opin Cell Biol 2000;12:174–179. [PubMed: 10712916]

Van Staveren WC, Steinbusch HW, Markerink-van Ittersum M, Repaske DR, Goy MF, Kotera J, Omori K, Beavo JA, de Vente J. mRNA expression patterns of the cGMP-hydrolyzing phosphodiesterases

types 2, 5, and 9 during development of the rat brain. J Comp Neurol 2003;467:566–580. [PubMed: 14624489]

Wiedenmann B, Franke WW. Identification and localization of synaptophysin, an integral membrane glycoprotein of Mr 38,000 characteristic of presynaptic vesicles. Cell 1985;41:1017–1028. [PubMed: 3924408]

Wilson, CJ. Basal ganglia. In: Sheperd, GM., editor. The synaptic organization of the brain. 4th edition. Oxford University Press; New York: 1998. p. 329-376.

NIH-PA Author Manuscript

NIH-PA Author Manuscript

NIH-PA Author Manuscript

NIH-PA Author Manuscript

NIH-PA Author Manuscript

NIH-PA Author Manuscript

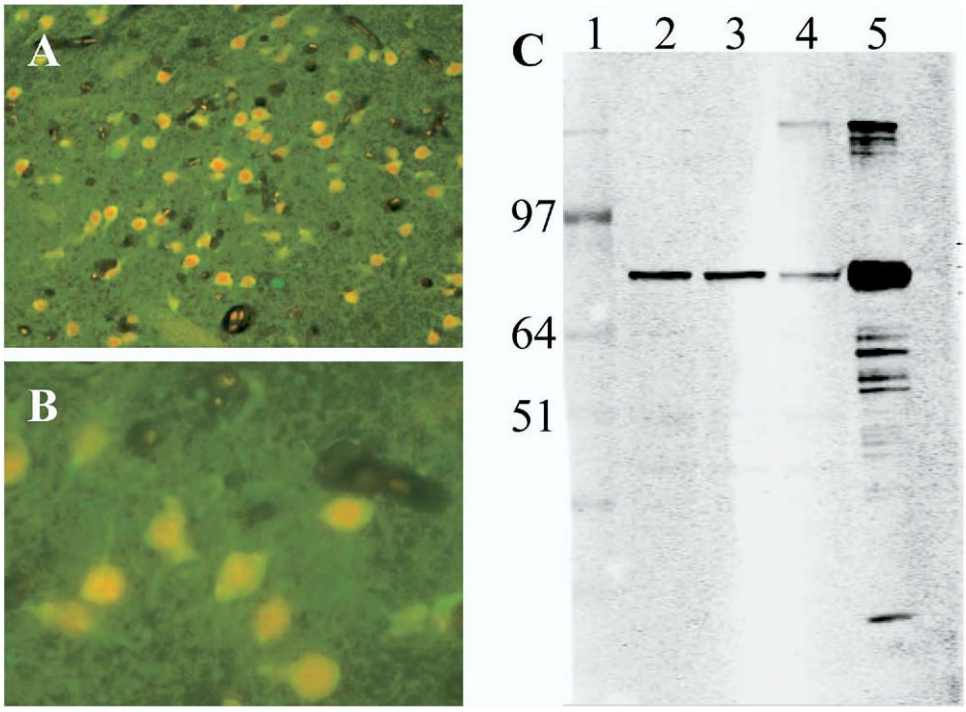

Fig. 1.

(A, B) Localization of PDE10A and DARPP-32 in striatum of cynomolgus monkey. Sections of cynomolgus monkey were stained sequentially with antibodies to PDE10A (green) and DARPP-32 (red) as described in Experimental Procedures. Images were merged and overlap between PDE10A and DARPP-32 is shown in yellow. Two sections are shown: A, magnification 20×; B, magnification 60×. (C) Western blot of striatal extracts from two cynomolgus monkeys (lanes 2 and 3) and rat (lane 4) stained for PDE10A-ir with 24F3.F11. Equal amounts of striatal extracts were loaded. Rat recombinant PDE10A is shown as a comparator (lane 5) and molecular weight markers are in lane 1.

NIH-PA Author Manuscript
NIH-PA Author Manuscript
NIH-PA Author Manuscript

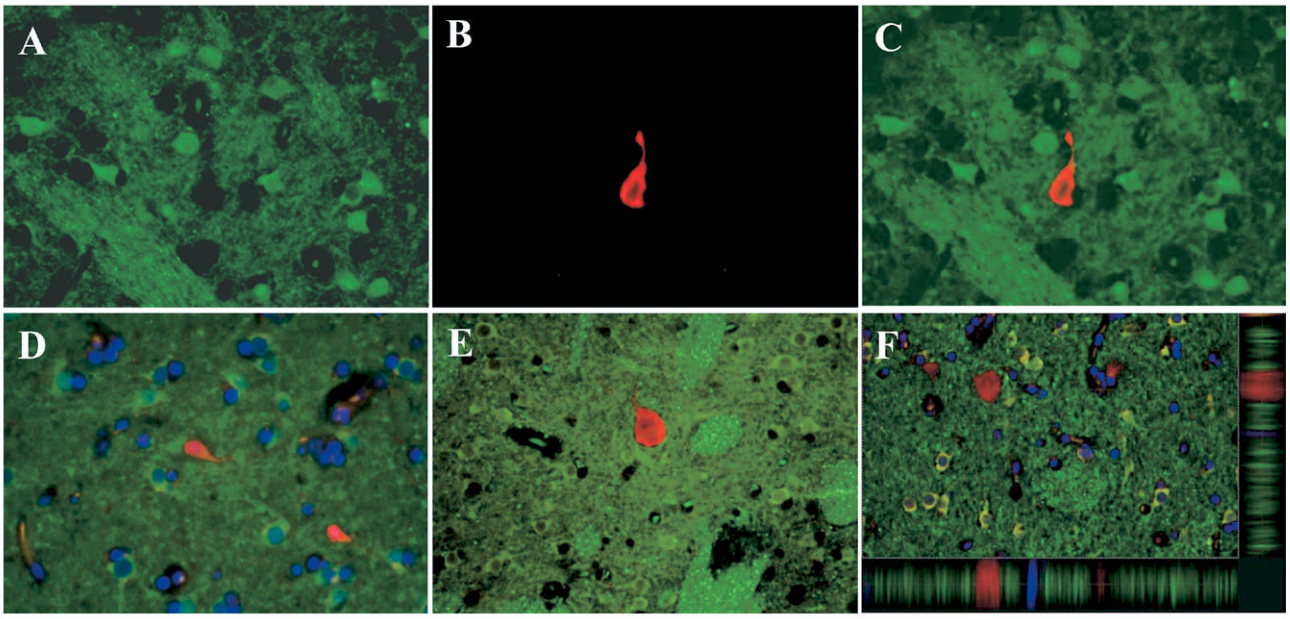

Fig. 2.

Localization of PDE10A, nNOS, calretinin, ChAT, and parvalbumin in striatum of cynomolgus monkey. Sections of cynomolgus monkey were stained sequentially with antibodies to PDE10A (A, C-F) and nNOS (B, C), calretinin (D), ChAT (E), parvalbumin (F) as described in Experimental Procedures. Images were merged (C, PDE10A/ nNOS, D, PDE10A/calretinin, E, PDE10A/ChAT, F, PDE10A/parvalbumin) and no overlap was detected between PDE10A and the other makers. In F, lines in the *x* and *y* axis mark points of interest. The intensity of the immunoreactive signal at each point along these lines is depicted on the bottom and right hand sides of the figure. Magnification 20×.

NIH-PA Author Manuscript

NIH-PA Author Manuscript

NIH-PA Author Manuscript

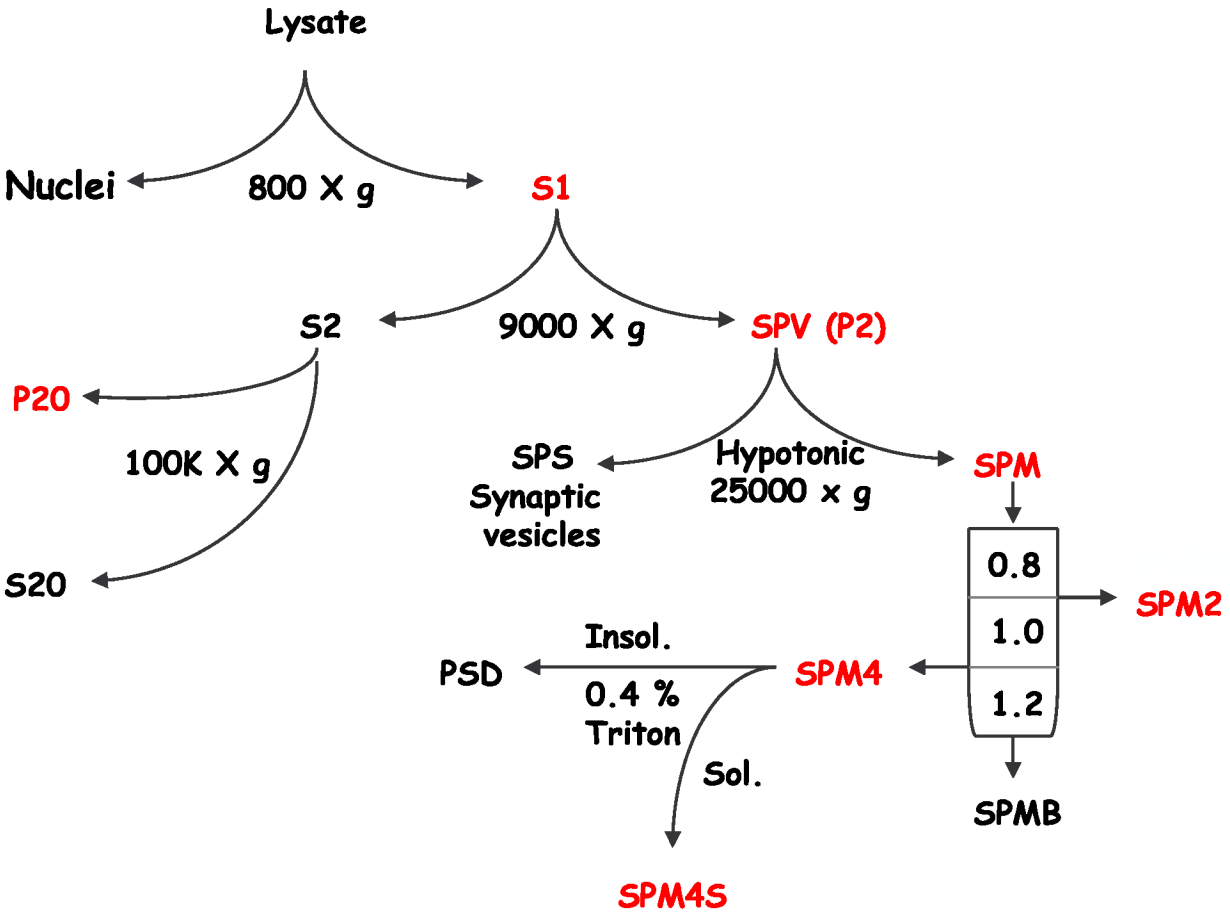

Fig. 3.

Schematic outline of subcellular fractionation sequence. See Experimental Procedures for full description of different fractions. Red, fractions containing substantial PDE10A-ir, black, fractions with little or no detectable PDE10A-ir.

NIH-PA Author Manuscript

NIH-PA Author Manuscript

NIH-PA Author Manuscript

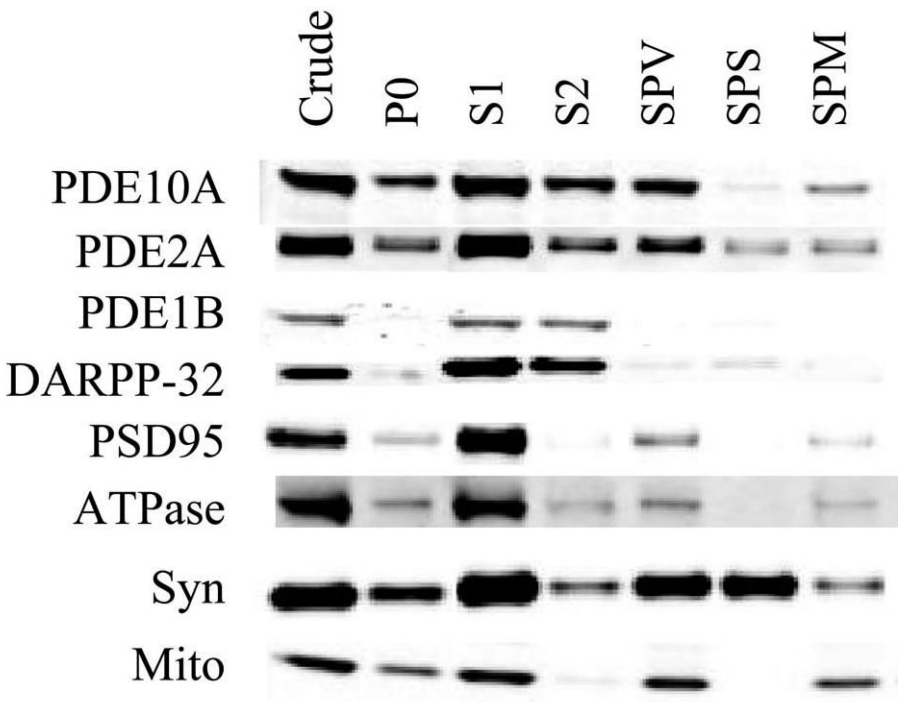

Fig. 4.

Western blot analysis of subcellular fractions from rat striatum with detection using a LiCor Odyssey. Fractions indicated at the top of the figure and antigens indicated on the left are described in Experimental Procedures.

NIH-PA Author Manuscript

NIH-PA Author Manuscript

NIH-PA Author Manuscript

Fig. 5.

Western blot analysis of SPM fractions from rat striatum with detection using a LiCor Odyssey. Fractions indicated at the top of the figure and antigens indicated on the left are described in Experimental Procedures.

NIH-PA Author Manuscript

NIH-PA Author Manuscript

NIH-PA Author Manuscript

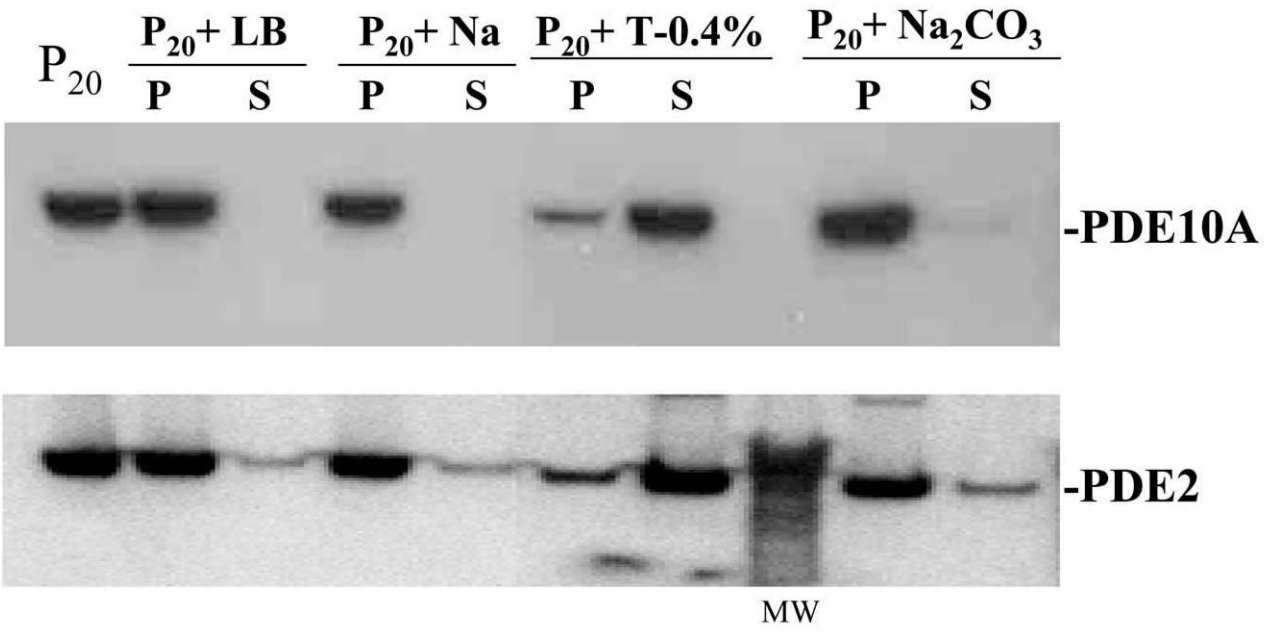

Fig. 6.

Western blot analysis of PDE10A association with the high speed membrane fraction with ECL Detection System. P20, the 100,000×g membrane fraction as indicated in Fig. 3; LB, lysis buffer; Na, 1 M NaCl; T-0.4%, 0.4% Triton X-100; Na_2CO_3,0.1MNa_2CO_3; P, pellet; S, supernatant.

NIH-PA Author Manuscript
NIH-PA Author Manuscript
NIH-PA Author Manuscript

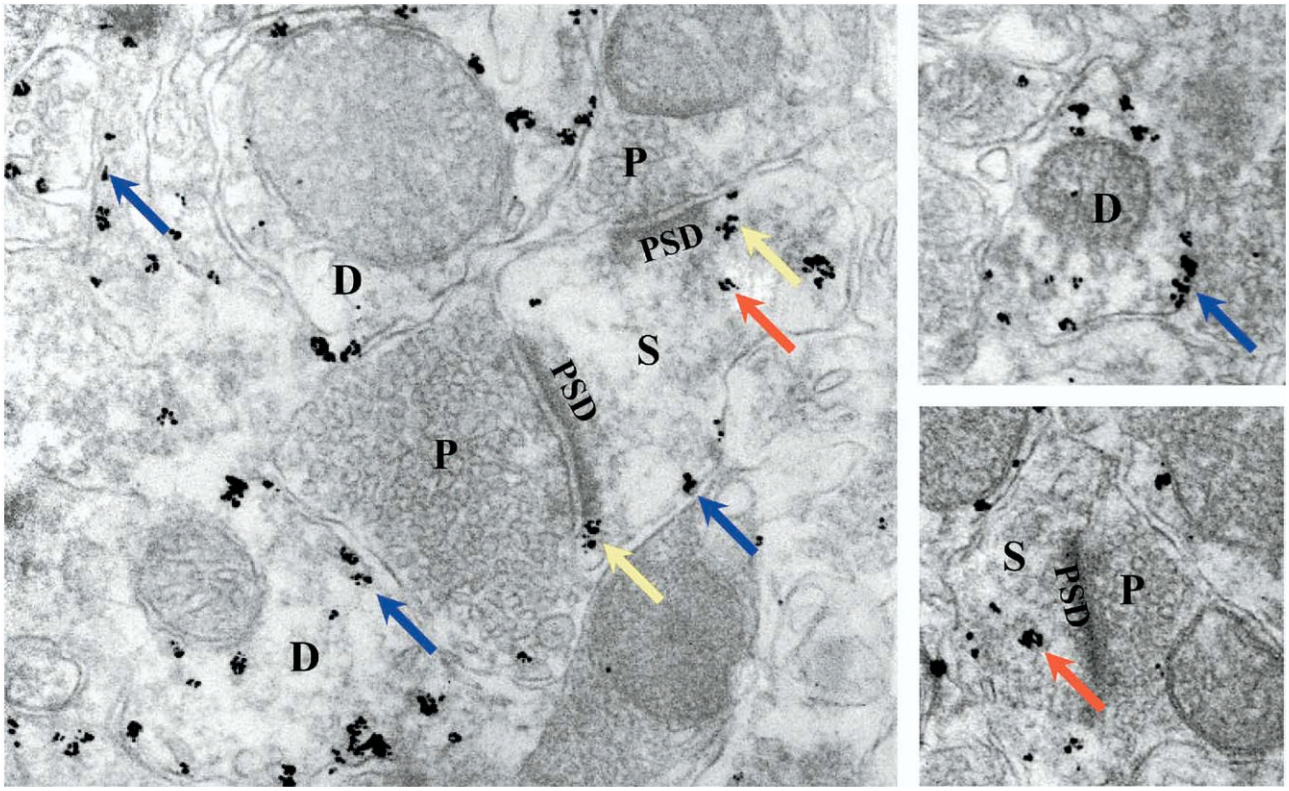

Fig. 7.

Localization of PDE10A in rat striatum by immuno-electron microscopy. Gold particles (black dots) represent PDE10A-ir. D, dendrite; P, vesicle-filled presynaptic terminal; S, spine. Blue arrows, PDE10A-ir apposed to dendritic and spine membranes, red arrows, PDE10A-ir within spines not apparently apposed to membranes, yellow arrows, PDE10A-ir at the edges of the PSD.